Physics Letters A 374 (2010) 3987–3990

Contents lists available at ScienceDirect

Physics Letters A

www.elsevier.com/locate/pla

Short-range interacting skyrmion charges in the long-range interacting skyrmion lattice

Qi Li *

Center of Theoretical Physics, Department of Physics, Capital Normal University, Beijing 100048, People's Republic of China

ARTICLE INFO

Article history:
Received 25 May 2010
Received in revised form 21 July 2010
Accepted 26 July 2010
Available online 3 August 2010
Communicated by A.R. Bishop

Keywords:
Skyrmion
Spectral method
p-Wave superconductivity
Nonlinear ordinary differential equation

ABSTRACT

A topological excitation-skyrmion in p-wave superconductors is studied in the context of Landau–Ginzburg–Wilson (LGW) theory. Interaction between skyrmion charge densities is shown to be short ranged from a derived effective field model. The computed energy per single skyrmion of skyrmion lattice suggests a long ranged lattice interaction.

1. Introduction

Spin triplet p-wave superfluid phase of fermion systems, for instance, ^{3}He, support a lot of topological excitations [1]. Due to the nature of the multi-component order parameter of the p-wave pairing symmetry, it is possible to have different symmetry broken phases and different topological excitations subjecting to various boundary conditions. Among these topological excitations, a well-known singular quantized vortex which has a core where the order is destroyed but the phase of the order parameter is continuous can be characterized by an integer valued winding number with a singular topological charge density. However, in the rotating superfluid ^{3}He, in addition to the singular quantized vortex, there is also a continuous topological texture which can trap 2 quanta of circulation [2,3] with a continuous distribution of topological charge density. This same situation may occur in the p-wave superconductors. Such additional kind of topological excitation can be stabilized in the presence of an external magnetic field $\boldsymbol{H}$ in a range $H_{c1} < |\boldsymbol{H}| < H_{c2}$ between a lower critical field H_{c1} and an upper critical field H_{c2} in the strong type II case. It is pointed out by Knigavko et al. [4] and they refer to this kind of continuous topological texture as a skyrmion. It is expected that skyrmions would form a periodic structure-skyrmion flux lattice just as singular vortex does in the sufficiently strong magnetic field [5,6]. In this case every single skyrmion in the area of a unit cell would trap 2 quanta of magnetic flux and the order parameters would smoothly match at the unit cell perimeters. Considering recently discovered candidates of p-wave superconductors, for instance, quasi 2D ruthenate Sr_2RuO_4 [7] and $Na_xCoO_2{\cdot}yH_2O$ [8], it is interesting to investigate the properties of skyrmions and the lattice they might form. More specifically, the nature of interaction between the skyrmion charges and the lattice they form should be identified. These properties are helpful to distinguish them from the traditional Abrikosov flux lattice [6,9].

In this Letter, firstly, to address the nature of the interaction between skyrmion charges, we will derive an effective field theory which can describe skyrmions in p-wave superconductors at the lower critical field and we will explicitly show the interaction between the charge of the skyrmions is short-ranged. Secondly, we will apply a numerical method-spectral method [10] to compute the energy of a single skyrmion with finite size R in circular cell approximation [11]. We will show that the energy per skyrmion has a strong dependence on the lattice constant R. In the large R limit, the leading $1/R$ dependence is consistent with the result by Knigavko et al. [4] but with a slightly larger coefficient. This is the signature that the interaction between the skyrmion lattice is actually long-ranged.

2. Effective model of p-wave superconductors

The order parameter of a triplet superconductor takes a matrix form [12]

$$\boldsymbol{\Delta}(\boldsymbol{k}) = \begin{bmatrix} -d_1(\boldsymbol{k}) + id_2(\boldsymbol{k}) & d_3(\boldsymbol{k}) \\ d_3(\boldsymbol{k}) & d_1(\boldsymbol{k}) + id_2(\boldsymbol{k}) \end{bmatrix} \tag{1}$$

* Tel./fax: +86 10 68903467.
E-mail address: qihlih@gmail.com.

0375-9601/$ – see front matter © 2010 Elsevier B.V. All rights reserved.
doi:10.1016/j.physleta.2010.07.070

with $\boldsymbol{k}$ the momentum. This gap matrix $\boldsymbol{\Delta}(\boldsymbol{k})$ has been parameterized by a three-component complex vector function $\boldsymbol{d}(\boldsymbol{k})$. One of the possible $\boldsymbol{d}(\boldsymbol{k})$ takes the following form,

$$\boldsymbol{d}(\boldsymbol{k}) = \Delta_0 \hat{\boldsymbol{e}}(\hat{\boldsymbol{m}} + i\hat{\boldsymbol{n}}) \cdot \boldsymbol{k} \tag{2}$$

Here, $\hat{\boldsymbol{e}}$ is a unit constant vector in spin space, where $\hat{\boldsymbol{m}}$ and $\hat{\boldsymbol{n}}$ are orthogonal constant unit vectors in the orbit space with Δ_0 the magnitude of the order parameter. This kind of parameterization corresponds to the Anderson–Brinkman–Morel (ABM) state of the superfluid phase of ^{3}He or β phase if we exchange the index of spin and orbit. In the following discussion, we will treat the magnitude of the $\boldsymbol{d}(\boldsymbol{k})$ vector Δ_0 to be a constant meaning the system is deep inside the superconducting state or when the superconductors are close to the H_{c1} where this treatment (London approximation) applies. In the later case, Δ_0 can only vary rapidly in a relatively small core whose length scale is set by the coherence length $\xi = 1/\sqrt{2m|t|}$ with m as the mass of the Cooper pair and t as the coefficient of the quadratic term of Ginzburg–Landau free energy density [9]. If we assume the spin degree freedom is freezed, namely $\hat{\boldsymbol{e}}$ points to a specific direction everywhere but $\boldsymbol{m}$ and $\boldsymbol{n}$ can fluctuate from their optimal directions, then the LGW action density can be written in a natural unit ($\hbar = c = 1$)

$$\mathcal{L}_{\mathrm{L}} = \frac{1}{2}(\partial_i \hat{\boldsymbol{l}})^2 + (\hat{\boldsymbol{n}}\partial_i \hat{\boldsymbol{m}} - a_i)^2 + \boldsymbol{b}^2 \tag{3}$$

with magnetic induction $\boldsymbol{b} = \nabla \times \boldsymbol{a}(\boldsymbol{r})$ and $\boldsymbol{a}(\boldsymbol{r})$ as the reducted vector potential. Here, a triad coordinate has been introduced by the relationship $\hat{\boldsymbol{l}}(\boldsymbol{r}) = \hat{\boldsymbol{n}}(\boldsymbol{r}) \times \hat{\boldsymbol{m}}(\boldsymbol{r})$. The differential with respect to the coordinate can be in the 3D space. In the following discussion, for simplicity, we will ignore the z dependence of all the fields. This corresponds to a perfect straight line structure in a bulk sample or a quasi 2D superconducting film. It should be noted that we have introduced dimensionless quantities by measuring distances in units of penetration depth $\lambda = \sqrt{m/4\pi q^2 \langle \Delta_0 \rangle^2}$ with q the charge of the Cooper pair and the action in units of $\Phi_0^2/32\pi^3\lambda$, and we introduce a dimensionless vector potential $\boldsymbol{a} = 2\pi\lambda \boldsymbol{A}/\Phi_0$, with $\Phi_0 = 2\pi/q$ the magnetic flux quantum.

The first term in Eq. (3) is identified as the $O(3)$ nonlinear sigma model which can support nontrivial topological excitations. However, this term is scale invariant which means the excitation with fixed energy has no stable size [13]. Although Eq. (3) looks very complicated, the number of independent fields of the optimal field configurations is only 2. This can be seen as follows. Orthogonal unit vectors $\hat{\boldsymbol{l}}$, $\hat{\boldsymbol{m}}$ and $\hat{\boldsymbol{n}}$ form a triad coordinate and thus number of independent components of these fields is 3. In the presence of the flux quantization condition, vector potential $\boldsymbol{a}$ has only 1 independent component. The two saddle point equations whose solution minimizes action density Eq. (3) will further reduce independent components by 2. This will make overall number of independent components to be 2. To see this point more explicitly, we will derive an effective field theory in terms of $\hat{\boldsymbol{l}}$ only as the follows.

We now are looking for saddle-point solutions to Eq. (3). Considering $\hat{\boldsymbol{l}}$ and $\boldsymbol{a}$ independent variables, and minimize Eq. (3) with respect to $\hat{\boldsymbol{l}}$ subject to the constraints $\hat{\boldsymbol{l}}^2 = \hat{\boldsymbol{n}}^2 = 1$ and $\hat{\boldsymbol{l}} \cdot \hat{\boldsymbol{n}} = 0$ yields

$$\nabla^2 \hat{\boldsymbol{l}} - \hat{\boldsymbol{l}}\big(\hat{\boldsymbol{l}} \cdot \nabla^2 \hat{\boldsymbol{l}}\big) + 2J_i(\hat{\boldsymbol{l}} \times \partial_i \hat{\boldsymbol{l}}) = 0 \tag{4a}$$

with

$$\boldsymbol{J} = \nabla \times \boldsymbol{b} \tag{4b}$$

the supercurrent. The derivative with respect to $\boldsymbol{a}$ is straightforward and yields a generalized London equation,

$$a_i + J_i = \hat{\boldsymbol{n}}\partial_i \hat{\boldsymbol{m}} \tag{4c}$$

By assuming Coulomb gauge, the above set of equations can be rewritten

$$b_i - \nabla^2 b_i = \frac{1}{2}\epsilon_{ijk}\hat{\boldsymbol{l}} \cdot (\partial_j \hat{\boldsymbol{l}} \times \partial_k \hat{\boldsymbol{l}}) \tag{5a}$$

$$\nabla^2 \hat{\boldsymbol{l}} - \hat{\boldsymbol{l}}\big(\hat{\boldsymbol{l}} \cdot \nabla^2 \hat{\boldsymbol{l}}\big) + 2\epsilon_{ijk}\partial_j b_k(\hat{\boldsymbol{l}} \times \partial_i \hat{\boldsymbol{l}}) = 0 \tag{5b}$$

It should be noted to obtain Eq. (5a), we have applied Mermin–Ho relation [14]. By assuming the magnetic induction points to the z direction, the right-hand side of Eq. (5a) is $\hat{\boldsymbol{l}}$ field dependent only and let it be referred as $4\pi Q(\boldsymbol{x})$. A further inspection of the expression of $Q(\boldsymbol{x})$ shows that it measures how fast the coordinate space R_2 is wrapped onto a unit sphere $\hat{\boldsymbol{l}}^2 = 1$ and thus related to a winding number or topological charge density [13]. It is straightforward to express all the $\boldsymbol{b}$ dependence in Eq. (3) by the $\hat{\boldsymbol{l}}$ from the relationship Eq. (5a). The result is very similar to the baby skyrmion model in quantum hall ferromagnets [15] which has a long-range interaction between topological charge densities,

$$\mathcal{L}_{\mathrm{L}} = \frac{1}{2}(\partial_i \hat{\boldsymbol{l}})^2 + \int d^2\boldsymbol{r}'\, Q(\boldsymbol{r}) Q(\boldsymbol{r}') V(\boldsymbol{r} - \boldsymbol{r}') \tag{6}$$

Here, the inter charge density potential V takes a form of a modified Bessel function of the second kind $8\pi I_0(r)$. It is not surprising to see this result because if we fixed $\hat{\boldsymbol{l}}$, then the topological charge density will naturally recover to a singular Dirac δ function, which leads to the familiar vortex flux case. This means in the case of large separation, the skyrmion charge has a short-range interaction just as the vortex does. It should be noted that the interaction between skyrmion charges is repulsive, thus skyrmions could form a lattice structure in the equilibrium state. It means every skyrmion in the lattice state prefers an equilibrium size R. This length scale has also to be determined by the flux quantization condition and thus related to the external field. To correctly account for this effect, Eq. (6) has to include the Zeeman energy-coupling between the magnetic induction and the external field. We will show how the skyrmion size is determined in the following section.

3. Single skyrmion energy in a lattice structure with a lattice constant *R*

It is difficult to directly analyze the skyrmion lattice configuration form Eq. (6). We will approximate the unit cell of a skyrmion lattice with hexagonal or square symmetry by an inscribed circle. In another word, we are looking for a $\hat{\boldsymbol{l}}$ profile which possesses cylindrical symmetry. To minimize the free energy, from Eq. (6), $\hat{\boldsymbol{l}}$ has to point to a specific direction at large distance. We assume this direction to be z direction. Due to the definition of topological charge density $Q(\boldsymbol{x})$ which is related to the stereographic projection, $\hat{\boldsymbol{l}}$ has to point $-z$ direction at the origin. Then we can define the angle between the z direction and $\hat{\boldsymbol{l}}$ to be $\theta(r)$. We will follow the parameterization of the fields from Knigavko et al. [4],

$$\begin{aligned}
\hat{\boldsymbol{l}} &= \hat{\boldsymbol{e}}_z \cos\theta(r) + \hat{\boldsymbol{e}}_r \sin\theta(r) \\
\hat{\boldsymbol{n}} &= \big(\hat{\boldsymbol{e}}_z \sin\theta(r) - \hat{\boldsymbol{e}}_r \cos\theta(r)\big)\sin\varphi + \hat{\boldsymbol{e}}_\varphi \cos\varphi \\
\hat{\boldsymbol{m}} &= \big(\hat{\boldsymbol{e}}_z \sin\theta(r) - \hat{\boldsymbol{e}}_r \cos\theta(r)\big)\cos\varphi - \hat{\boldsymbol{e}}_\varphi \sin\varphi \\
\boldsymbol{a}(\boldsymbol{x}) &= a(r)\hat{\boldsymbol{e}}_\varphi
\end{aligned} \tag{7}$$

where φ is the polar angle. Such parametrization has the property that at the perimeter ($\theta = 0$), the winding angle in $\boldsymbol{n}$ and $\boldsymbol{m}$ of Eq. (7) is 2φ instead of φ. This means every skyrmion traps $2\Phi_0$ flux.

With this parameterization, from Eq. (3), we obtain the energy per unit length, along the cylinder axis, in a region of radius R,

$$E/E_0 = \frac{1}{2}\int_0^R dr\,r\left[\left(\theta'(r)\right)^2 + \frac{1}{r^2}\sin^2\theta(r)\right] + \int_0^R dr\,r\left[\frac{1}{r}\left(1+\cos\theta(r)\right)+a(r)\right]^2 + \int_0^R dr\,r\left[\frac{a(r)}{r}+a'(r)\right]^2 \tag{8}$$

Here, $E_0 = (\Phi_0/4\pi\lambda)^2$ is a basic unit measure of the energy. The energy has been expressed by two independent fields, $\theta(r)$ and $a(r)$ and a free parameter R which will be identified as the lattice constant latter. These have to be determined from the saddle point equations and boundary conditions. Take the functional derivatives of E with respect to $\theta(r)$ and $a(r)$ yields Euler–Lagrange equations

$$\theta''(r) + \frac{1}{r}\theta'(r) = \frac{-\sin\theta(r)}{r}\left[\frac{2+\cos\theta(r)}{r} + 2a(r)\right] \tag{9a}$$

$$a''(r) + \frac{1}{r}a'(r) - \frac{1}{r^2}a(r) = a(r) + \frac{1}{r}\left[1+\cos\theta(r)\right] \tag{9b}$$

To solve above coupled nonlinear ordinary differential equations (ODEs) with boundary conditions $\theta(r=0)=\pi$ and $\theta(r=R)=0$, $a(r=0)=0$ and $a(r=R)=\frac{1}{\pi R}$, we apply a numerical method referred as the spectral method [10]. The basic idea of this method is to expand the wanted functions by Chebyshev polynomials with unknown coefficients. For any desired orders of numerical precision, we truncate the polynomials at an appropriate order N. For instance, in our following calculation, we fixed the maximal order of polynomial to be $N = 40$. This means there are overall $2N$ unknown coefficients of $\theta(r)$ and $a(r)$ to be determined. Then we can pick up $N-2$ collocation points by Galerkin method in between the two end points and evaluate the wanted functions at these points. Adding the boundary conditions, there are $2N$ nonlinear algebraic functions for the $2N$ unknown variables. With the help of the sophisticated root finding software, the coefficients can be easily obtained.

After solving Euler–Lagrange equations, we calculate the free energy of a skyrmion with different size R from Eq. (8). In Fig. 1 we show the size dependence of a skyrmion energy. In the range of R from 100 to 300, the best $1/R$ fit takes the form

$$E/E_0 = 2 + 6.67/R - 7.9\frac{\ln R}{R^2} - 1.2/R^2 \tag{10}$$

Comparing this numerical result to what we got in Ref. [9] where the skyrmion energy is expanded in terms of the skyrmion size R,

$$E/E_0 = 2 + \frac{8\sqrt{6}}{3}\frac{1}{R} - \frac{16}{3}\frac{\ln R}{R^2} - \frac{4}{45}\left[7+30\ln(3/2)\right]\frac{1}{R^2} \tag{11}$$

we can clearly see our numerical result at large R is consistent with our analytic perturbative result.

It should also be noted that our calculation of the skyrmion energy has two dominant pieces. The constant piece is for the scale invariant nonlinear σ O(3) term in Eq. (6) and the next leading order term is proportional to $1/R$ which implies a nature of long-ranged repulsive interaction between skyrmion *lattice* [9].

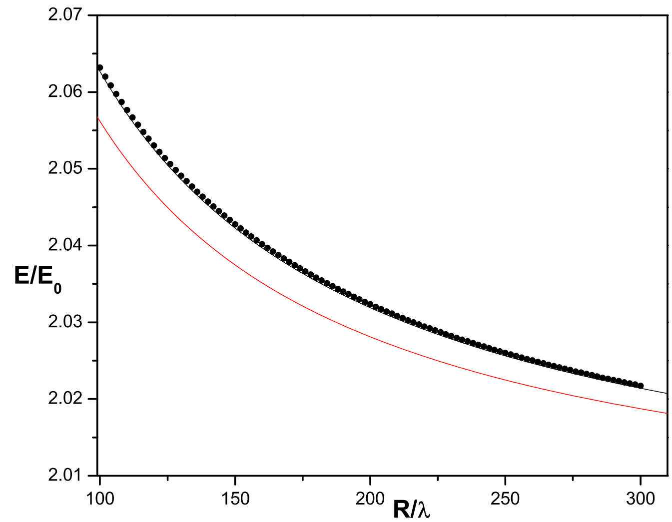

Fig. 1. Skyrmion energy vs. its size R. Black data points are the skyrmion energy computed from the spectral method. Black line is plotted from Eq. (11) and is indistinguishable from the numerical fitting by Eq. (10) in the plot range. To manifest the fact that data points lie slightly above the fitting curve by Ref. [4] we plot it as the red line for eye guidance. (For interpretation of the references to color in this figure legend, the reader is referred to the web version of this Letter.)

This should be distinguished from the nature of the short-range repulsive interaction between the topological charge density.

So far, we have introduced a free parameter-R-size of a skyrmion and we will determine its value by the Gibbs free energy which describes the skyrmion energy in the external field $\boldsymbol{h}$. To do this, the Zeeman term $-2\boldsymbol{h}\cdot\boldsymbol{b}$ in the dimensionless unit has to be added in Eq. (3) and Eq. (6). It is obvious that the topological charge interaction term favors large sized skyrmions whereas the Zeeman term favors small sized ones. This competition will lead to the non-analytic term in Eq. (11). In the large R case, we keep only the first two terms in Eq. (11) and get the equilibrium size of a skyrmion in terms of the most significant physical quantities H

$$R_0 = 2\sqrt{6}\lambda/\Delta, \tag{12}$$

where $\Delta \equiv H/H_{c1} - 1$ and $H_{c1} = \Phi_0/4\pi\lambda^2$. For extreme type II superconductors, the required external field H_{c1} to penetrate the first couple of fluxes into the superconducting sample is smaller than the one for the traditional vortex. Thus extreme type II p-wave superconductors favor skyrmions. Compared to the well-known result of vortex flux at H_{c1} [6], skyrmions are much more difficult to generate. In the magnetization curve b vs. Δ, this effect will show a much flatter slope than the vortex case does. As a consequence, this long-ranged interaction between the skyrmion lattice makes the lattice much more stable than the Abrikosov flux lattice.

4. Conclusions

In summary, we have derived an effective field theory to describe a low energy excitation-skyrmion in p-wave superconductors at the lower critical field. We also solved the skyrmion configurations numerically. The result of energy of different skyrmion sizes in the large R case is excellently consistent with our previous analytic result.

It is interesting to notice that the neutron scattering experiment on Sr_2RuO_4 [16] indicates the magnetic induction profile does not match that of the traditional Abrikosov lattice. It is also reported the magnetic induction decays much slower with reciprocal lattice vector than the s-wave GL value. These evidence suggest a skyrmion lattice theory or the half-quantum flux lattice [17] theory might be relevant to give the explanation.

Acknowledgements

Qi Li is grateful to the helpful discussions with D. Belitz and J. Toner. This work is supported in part by an initiative start-up funds from the Capital Normal University. It is also supported by National Keystone Basic Research Program (973 Program) under Grant No. 2007CB310408.

References

[1] O.V. Lounasmaa, E. Thuneberg, Proc. Natl. Acad. Sci. 96 (1999) 7760.
[2] P.J. Hakonen, O.T. Ikkala, S.T. Islander, Phys. Rev. Lett. 49 (1982) 1258.
[3] H.K. Seppälä, G.E. Volovik, J. Low. Temp. Phys. 51 (1983) 279.
[4] A. Knigavko, B. Rosenstein, Y.F. Chen, Phys. Rev. B 60 (1999) 550.
[5] D. Saint-James, G. Sarma, E.J. Thomas, Type II Superconductivity, Pergamon Press, Oxford, 1969.
[6] M. Tinkham, Introduction to Superconductivity, McGraw–Hill, New York, 1975.
[7] Y. Maeno, H. Hashimoto, K. Yoshida, S. Nishizaki, T. Fujita, J.G. Bednorz, F. Lichtenberg, Nature 372 (1994) 532.
[8] I. Mazin, M. Johannes, Nat. Phys. 1 (2005) 91.
[9] Q. Li, J. Toner, D. Belitz, Phys. Rev. B 79 (2009) 014517.
[10] J.P. Boyd, Chebyshev and Fourier Spectral Methods, Springer, Berlin, 1989.
[11] W.V. Pogosov, K.I. Kugel, A.L. Rakhmanov, E.H. Brandt, Phys. Rev. B 64 (2001) 064517.
[12] D. Vollhardt, P. Wölfle, The Superfluid Phases of Helium 3, Taylor & Francis, 1990.
[13] R. Rajaraman, Solitons and Instantons, North-Holland, Amsterdam, 1982.
[14] N.D. Mermin, T.-L. Ho, Phys. Rev. Lett. 36 (1976) 594.
[15] S.L. Sondhi, A. Karlhede, S.A. Kivelson, E.H. Rezayi, Phys. Rev. B 47 (1993) 16419.
[16] P.G. Kealey, T.M. Riseman, E.M. Forgan, L.M. Galvin, A.P. Mackenzie, S.L. Lee, D.M. Paul, R. Cubitt, D.F. Agterberg, R. Heeb, Z.Q. Mao, Y. Maeno, Phys. Rev. Lett. 84 (2000) 6094.
[17] S.B. Chung, D.F. Agterberg, E.-A. Kim, New J. Phys. 11 (2009) 085004.